Mattei L, DiPuccio F, Joyce TJ, Ciulli E.

Effect of size and dimensional tolerance of reverse total shoulder prosthesis on wear: An in-silico study.

***Journal of the Mechanical Behavior of Biomedical Materials* 2016, 61, 455-463.**

Effect of size and dimensional tolerance of reverse total shoulder arthroplasty on wear: an in-silico study

Lorenza Mattei[1*], Francesca Di Puccio[1], Thomas J. Joyce[2], Enrico Ciulli[1]

[1]Department of Civil and Industrial Engineering, Largo Lucio Lazzarino 2, Pisa, 56126, IT

[2]School of Mechanical and Systems Engineering, Stephenson Building, Claremont Road, Newcastle upon Tyne, NE1 7RU, UK

Abstract

Although huge research efforts have been devoted to wear analysis of ultra high molecular weight polyethylene (UHMWPE) in hip and knee implants, shoulder prostheses have been studied only marginally. Recently, the authors presented a numerical wear model of reverse total shoulder arthroplasties (RTSAs), and its application for estimating the wear coefficients *k* from experimental data. In this study, such models and *k* expressions are exploited to investigate the sensitivity of UHMWPE wear to implant size and dimensional tolerance. A set of 10 different geometries was analysed, considering nominal diameters in the range 36-42 mm, available on the market, and a cup dimensional tolerance of +0.2,-0.0 mm (resulting in a diametrical clearance ranging between 0.04-0.24 mm), estimated from measurements on RTSAs. Since the most reliable wear law and wear coefficient *k* for UHMWPE are still controversial in the literature, both the Archard law (AR) and the wear law of UHMWPE (PE), as well as four different *k* expressions were considered, carrying out a total of 40 simulations.

Results showed that the wear volume increased with the implant size and decreased with the dimensional tolerance for both wear laws. Interestingly, different trends were obtained for the maximum wear depth vs. clearance: the best performing implants should have a high conformity according to the AR law but low conformity for the PE law. However, according to both laws, wear is highly affected by both implant size and dimensional tolerance, although it is much more sensitive to the latter, with up to a twofold variation of wear predicted. Indeed, dimensional tolerance directly alters the clearance, and therefore the lubrication and contact pressure distribution in the implant. Rather surprisingly the role of dimensional tolerance has been completely disregarded in the literature, as well as in the standards. Furthermore, this study notes some important issues for future work, such as the validation of wear laws and predictive wear models and the sensitivity of *k* to implant geometry.

Keywords: reverse total shoulder arthroplasty, implant size, dimensional tolerance, wear modelling, wear law, UHMWPE.

1 Introduction

Reverse total shoulder arthroplasty (RSTA) is an accepted option to treat rotator cuff tears since their clinical outcomes are better than those of anatomical implants. Nevertheless, the literature reports a revision rate of RTSAsin the range 0%-22% at the short-medium term follow up (33-52 months) (Nam et al. 2010a). There are multiple causes of failure associated with shoulder prostheses. Fevang et al. (Fevang et al. 2009)

* Corresponding author
Tel. Number: (+39) 050 2228019
Email: l.mattei@ing.unipi.it

showed that aseptic loosening due to osteolysis was the main cause of revision of RTSA in Norway. Scapula notching is a recognized complication with RTSA. This may be linked with impingement but it has also been suggested that wear particles may contribute to it too (Nyffeler et al. 2004). This view has been restated recently as motivation for consideration of more wear resistant materials in shoulder arthroplasty (Peers et al. 2015). In addition, several types of wear damage, from pitting and edge deformation to abrasion and delamination, have been observed in retrieved components of RTSA (Nam et al. 2010b, Day et al. 2012, Dillon et al. 2015, Wiater et al. 2015). Therefore wear is a recognized factor in shoulder arthroplasty.

Although huge research efforts have been devoted to wear analysis/predictions of UHMWPE-on-metal hip and knee prostheses (Mattei et al. 2011, Mattei et al. 2013a, Mattei et al. 2013b), shoulder implants have gained interest only recently and require further studies. The causes of wear of RTSAshave been investigated mainly experimentally. In particular, the effect of some design characteristics on implant wear has been investigated, among which: the presence of a hole at the dome of the bearing cup surface due to the fixation screw (Vaupel et al. 2012), retentive vs non retentive profiles of the glenoid surface (Carpenter et al. 2015), the irradiation grade of UHMWPE (Peers et al. 2015) and the inversion of the bearing materials (Kohut et al. 2012). With the exception of the irradiation grade of UHMWPE, all the above mentioned factors revealed only a slight influence on the implant wear rates. Among the few numerical studies on wear of RTSAs, (Ribeiro et al. 2011) and (Quental et al. 2015) analysed the effect of the clearance and the glenoid lateral offset, respectively, but unfortunately the reliability of their results is limited because of the use of wear coefficients originally estimated for hip and knee implants, which have been shown to be much lower (up to -58%) than the shoulder wear coefficients (Mattei et al. 2016).

Actually, the influence of the implant geometry on RTSA wear has never been deeply investigated in the literature, although it certainly plays a major role as it directly affects the contact and lubrication conditions in addition to muscle force, joint load and range of motion (Langohr et al. 2015). In particular, as for a ball-in-socket joint, the most important geometrical features of RTSA are the cup/head diameter (d_c and d_h, respectively) and the diametrical clearance ($cl = d_c - d_h$), as demonstrated for hip implants (Leslie et al. 2008, Tudor et al. 2013). Commercially available RTSAs are said to have high conformity, therefore, they are usually characterized only by their nominal diameter d_n mainly within range 36–42 mm. However, for practical purposes, a certain diametrical mismatch between the cup and head must be guaranteed in order to preserve the lubrication of the surfaces. The value of the mismatch depends on design criteria as well as on the manufacturing processes. Therefore, while the dimensional tolerances of implant components are fundamental both for implant clinical outcomes and for wear investigations, they are generally not described in standards (e.g. ASTM F1378) or in research studies. Moreover, also the effect of the real geometry of RTSAs, i.e. measured d_h and d_c, has never, to the authors' best knowledge, been discussed in the literature. The only study that reports some theoretical values of *cl* is (Ribeiro et al. 2011), which simulated 36 mm RTSAs with *cl*=0, 0.02, 0.10 mm. It should be observed that *cl*=0 mm represents an ideal conformity between surfaces, which is practically an unrealistic configuration.

The aim of the present study was to numerically investigate the influence of implant size and dimensional tolerances on wear of RTSAs. Wear predictions were carried out using an analytical and parametric wear model presented by the authors in (Mattei et al. 2016). A set of 10 simulation geometries was considered, including different implant sizes, with d_n varying from 36 to 42 mm, and a cup dimensional tolerance in the range +0.2, -0.0 mm (resulting in *cl* ranging between 0.04-0.24 mm). On the other hand, the dimensional tolerance of the metallic head was considered negligible, as explained in §2.2.1. The values of dimensional tolerances were derived from measurements on five samples of RTSAs mentioned in (Smith et al. 2015, Mattei et al. 2016). Since the most reliable wear law/wear coefficient for metal-UHMWPE bearings is still controversial (Mattei et al. 2013b), each simulation case was carried out assuming both the Archard wear law and a wear law for UHMWPE proposed in (Liu et al. 2011), and four different expressions of the wear coefficient, specific for RTSAs (Mattei et al. 2016). Consequently, this study proposes a combined sensitivity

analysis (for a total of 40 simulations) of wear to implant geometry and wear laws/coefficients thus providing important suggestions for reducing RTSAs wear.

2 Materials and Methods

2.1 Wear modelling

The numerical wear model used in the present study was presented by the authors in (Mattei et al. 2016), consequently, only a brief description is provided herein.

The model was implemented in Mathcad® and its analytical and parametric formulation allows for easily simulating different implants and operating conditions. The implant is modelled as a glenoid spherical head articulating with a humeral cup fixed in the humeral bone by means of a metal back, with an orientation defined by the anteversion angle α and the inclination angle β (Fig.1).

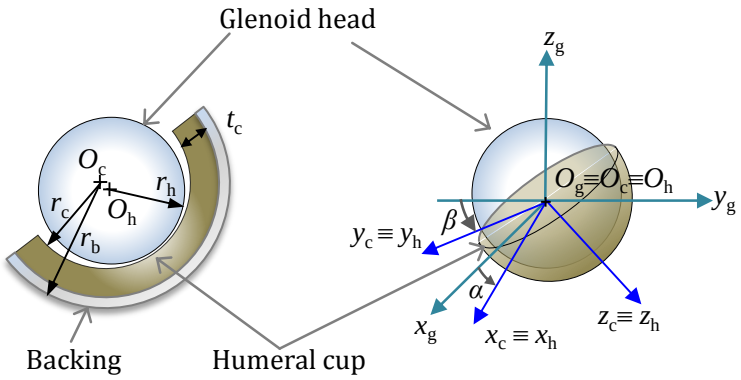

Fig.1. Model geometry (a) and coordinate frames in the reference configuration with no loading and null rotations (b). Note that r stands for radius, thus r_h=d_h/2 and r_c=d_c/2; r_b is the outer radius of the backing while t_c is the cup thickness.

Based on some simplifying hypotheses (e.g. head not affected by wear, no geometry update (Mattei et al. 2016)), the wear model quickly performs contact and kinematic analyses and thus predicts linear and volumetric wear according to both the Archard wear law (AR) and the wear law for UHMWPE (PE), also accounting for the cross-shear phenomenon. The wear laws were implemented in the local instantaneous form, in terms of linear wear rate $\dot{h}$ at a given point P after a duration t of the loading history, as follows:

$$\dot{h}_{\mathrm{AR}}(P,t) = k_{\mathrm{AR}}(P,t)\; p(P,t)\,\left|\mathbf{v}(P,t)\right| \tag{1}$$

$$\dot{h}_{\mathrm{PE}}(P,t) = k_{\mathrm{PE}}(P,t)\,\left|\mathbf{v}(P,t)\right| \tag{2}$$

where the subscript AR/PE indicates the wear law, $p(P,t)$ is the contact pressure and $\mathbf{v}(P,t)$ is the sliding velocity. One of the main difference between the two laws, consists in the role of the contact pressure which appears in Eq.(1) but not in Eq.(2): in fact, according to the AR law the wear rate depends on p, whilst, according to PE law it does not. Such important point has been largely discussed in the literature ((Liu et al. 2011, Mattei et al. 2013b)). Accordingly, the wear coefficients of Eqs. (1-2) are conceptually different, being k_{AR} a volume per work unit, whilst k_{PE} a dimensionless quantity. For each simulation case, three different expressions of k_{AR} were considered, i.e. K_{AR}, $k_{\mathrm{AR}}(CS)$, $k_{\mathrm{AR}}(CS, \bar{p})$, while only one for k_{PE}, i.e. $k_{\mathrm{PE}}(CS)$, where CS is the cross-shear (see (Mattei et al. 2016) and (Mattei et al. 2013b)) and $\bar{p}$ the average contact pressure over

a loading cycle. Such expressions are summarized in Table 1 and were estimated specifically for RTSAs with not-cross-linked PE cups in (Mattei et al. 2016).It is worth noting that *CS* only depends on the kinematic conditions, whilst $k_{AR}(CS, \bar{p})$ decreases with the contact pressure. Consequently, according to the AR law, the wear rate linearly increases with p for K_{AR} and $k_{AR}(CS)$, while changes non linearly with p for $k_{AR}(CS, \bar{p})$.Other inputs of the model are: the implant geometry and positioning, the material properties, the kinematic/loading conditions and the number of wear cycles to be simulated. Outputs include the local instantaneous contact pressure and the cross-shear ratio *CS* (defined according to (Mattei et al. 2013b)), the relative trajectories of contact points and the wear indicators, i.e. the volumetric wear and the wear map.

Table 1. Wear coefficients evaluated specifically estimated for RTSAs in (Mattei et al. 2016) for d_c=42.1 mm and *cl*=0.14 mm *and here assumed for numerical predictions.*

Type	Value/expression (mm³/(N m))
$\boldsymbol{K_{AR}}$	2.219×10^{-6}
$\boldsymbol{k_{AR}(CS)}$	$\begin{cases}(0.791\ln(CS)+3.9)10^{-6} & if\ 0.01\le CS\le 0.5\\ 0.2639\times10^{-6} & if\ 0\le CS\le 0.01\end{cases}$
$\boldsymbol{k_{AR}(CS,\bar{p})}$	$\begin{cases}2.2\,e^{(-13.1+0.19\ln(CS)-0.29\,\bar{p})} & if\ 0.01\le CS\le 0.5\\ 1.404\times10^{-6} & if\ 0\le CS\le 0.01\end{cases}$
$\boldsymbol{k_{PE}(CS)}$	$1.32\left[(8.5173\times10^{-65}+9.3652\times10^{-60}\,CS)^{1/6.7454}\right]$

2.2 Simulated cases

2.2.1 Geometry and materials

Wear predictions were carried out for 10 different implant geometries, as summarized in Table 2: the effect of the dimensional tolerance was investigated simulating 7 implants with the same nominal diameter and different clearance, whilst the effect of the implant size simulating 4 implants with the same clearance but different nominal diameter. It is worth noting that the case with d_c=42.1 mm and *cl*=0.14 mm was considered in both simulation groups.

In order to investigate the effect of the dimensional tolerance on wear, the geometrical characteristics of five 42 mm RTSAs (Mattei et al. 2016) were taken as a reference. The heads had an average diameter of 41.96 mm, with negligible deviations with respect to it (<0.05%), while the values of the cup diameter were in the range 42.00–42.20 mm, thus resulting a cup dimensional tolerance +0.20, +0.00 mm. Since the dimensional variations for the cup were one order of magnitude higher than the head one, only the former was considered in the sensitivity analysis of wear. Accordingly, simulations were carried out for implants all having the same d_h, i.e. 41.96 mm, while varying d_c in the range 42–42.2 mm, so that the diametrical clearance was assumed to be *cl*=0.04–0.24 mm (see Table 2).

In order to investigate the effect of the implant size, the following values of nominal diameter were considered: 36-38-40-42 mm, according to commercially available implants (see Table 1). Taking as a reference the dimensional tolerances discussed above, a deviation of 0.04 mm and 0.1 mm was assumed for the head and cup, respectively. Consequently, for an implant of nominal diameter d_n, it resulted d_h=d_n-0.04 mm and d_c=d_n+0.1 mm, so that all implants were characterized by the same clearance *cl*=(d_n+0.1)-(d_n-0.04)mm=0.14 mm (see Table 2).

Table 1. Summary of simulated implant geometries. A total of 10 simulations were carried out both to investigate the effect of implant dimensional tolerance and size. It is worth noting that the fourth and the last cases are the same. Legend: $d_{n,h,c}$=nominal/head/cup diameter; cl=diametrical clearance.

Investigation	d_n (mm)	d_h (mm)	d_c (mm)	cl (mm)
Effect of dimensional tolerance	42	41.96	42.00	0.04
			42.04	0.08
			42.08	0.12
			42.10	0.14
			42.12	0.16
			42.16	0.20
			42.20	0.24
Effect of implant size	36	35.96	36.10	0.14
	38	37.96	38.10	
	40	39.96	40.10	
	42	41.96	42.10	

In all cases, it was considered the humeral cup had a thickness of 7 mm and was made of not cross-linked UHMWPE (0 MRad), with an elastic modulus of 0.5 GPa and a Poisson coefficient of 0.4. It should be noted that the head was considered rigid.

2.2.2 Boundary conditions

The boundary conditions applied in the wear test described in (Mattei et al. 2016) were simulated. Accordingly, the cup, orientated horizontally (α=β=0°), was loaded vertically and subjected to inward-outward (IO) rotation, whilst the head was subjected to the sequence of flexion-extension (FE) and abduction-adduction (AA) rotation (Fig.2a). A typical daily task, i.e. a mug-to-mouth action, was simulated according to (Kontaxis 2010, Smith et al. 2015), corresponding to the angles and load in Figs.2b and c, respectively.

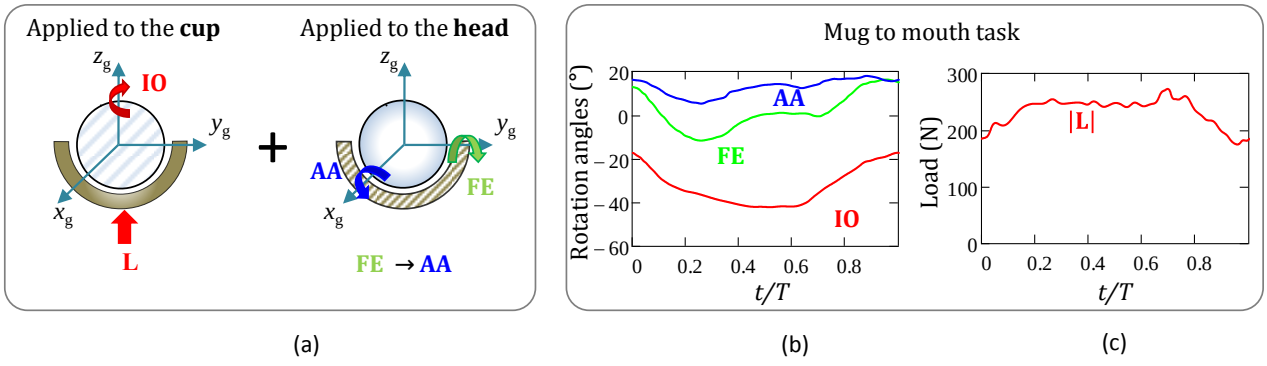

(a) (b) (c)

Fig.2. Boundary conditions: rotations/load applied to the implant components (a) and their temporal variation (b, c) for a mug-to-mouth task (Kontaxis 2010, Smith et al. 2015). Legend: FE: Flexion-Extension; AA: Abduction-Adduction; IO: inward-outward rotation, T: task/cycle period.

Simulations considered a total of 2 x10^6 working cycles and provided as results the wear volume V and the linear wear depth h. The latter was plotted as the wear distribution over the cup surface, and the result was characterized by a maximum value h_{max}.

3 Results

3.1 Effect of dimensional tolerance

The main results describing the effect of the dimensional tolerance, i.e. the diametrical clearance, on wear of a 42 mm implant, are reported in Figs.3-4.

Figure 3 shows the trend of the maximum wear depth h_{max} and the wear volume V with the diametrical clearance cl, assuming different wear laws/coefficients. It is worth noting that, moving from the left to the right of Fig.3, the higher the cl, the less conformal the contact. Results clearly showed the fundamental role played by the dimensional tolerance on wear rates, and how the latter are affected by the wear law/coefficient.

As far as the AR law is concerned, the effect of cl was demonstrated to affect significantly h_{max} and poorly V. In particular, as the cl increases, h_{max} increases (Fig.3a) whilst V slightly decreases (Fig.3b). A similar behavior was observed for K_{AR} and $k_{AR}(CS)$, since h_{max} increases almost linearly with cl, with a percentage variation of about +120% passing from cl=0.04 mm to cl=0.24 mm. In case of $k_{AR}(CS, \bar{p})$, h_{max} increases non linearly and more slowly with respect to K_{AR} and $k_{AR}(CS)$, with a percentage variation of h_{max} being almost half, i.e. +63%. On the other hand, for all the three types of k expressions, a slight linear decrease of the wear volume with cl was predicted, almost negligible change in K_{AR} and about of -9% and -19% for $k_{AR}(CS)$ and $k_{AR}(CS, \bar{p})$, respectively.

Wear predictions according to the PE wear law revealed a very different effect of the dimensional tolerance on wear, with respect to the AR law. Firstly, the cl appeared to affect V more than h_{max}. Secondly, as far as h_{max} is concerned, an opposite trend with respect to AR law was observed: as the cl increases, the h_{max} decreases from 0.112 mm to 0.093 mm, i.e. by about -17% (Fig.3a). On the other hand, the wear volume decreases with the cl as for the AR law, but the variation is non-linear and more significant (Fig.3b). Indeed, V decreases from 53.9 mm^3 to 23.8 mm^3, corresponding to a percentage variation of -56%.

It is worth noting that for all wear laws/coefficients, the wear volume estimated for the implant with d_c=42.1 mm and cl =0.14 mm was 26.6 mm^3. Indeed, as mentioned above, all expressions of k reported in Table 1 were estimated by simulating a wear test with an implant with such geometrical features (Mattei et al. 2016) and matching the numerical and experimental wear volumes.

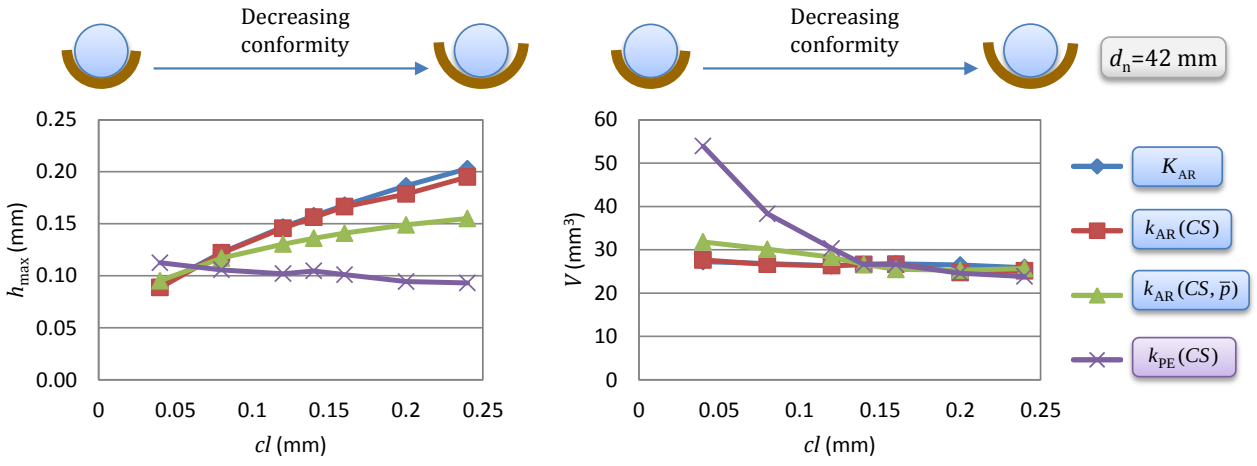

(a) (b)

Fig.3. Effect of diametrical clearance cl on (a) maximum wear depth h_{max} and (b) wear volume V for a 42 mm implant. Comparison of wear predictions for different wear laws and wear coefficients.

The influence of the dimensional tolerance/clearance on h_{max} and V, is clarified by the wear maps of Fig.4. In particular, it compares the wear maps (projected in x_c-y_c plane) of three different geometries characterized by the minimum, the average and the maximum value of clearance, i.e. 0.04 mm, 0.14 mm and 0.24 mm, respectively. As an example, results are reported for $k_{AR}(CS)$ (top row) and for $k_{PE}(CS)$ (bottom row). Indeed, results obtained for K_{AR} and $k_{AR}(CS, \bar{p})$ were very similar to those of $k_{AR}(CS)$. Both for the AR and PE law, Fig.4 shows that as the *cl* increases and the contact becomes less conformal, the contact/worn area results become smaller.

In agreement with the trends of Fig. 3, for the AR law the wear depth increases markedly with *cl* but, combined with a smaller worn area, a slightly lower V is predicted. In particular, when assuming K_{AR}, V results almost constant with *cl* since it is proportional to the work done by the frictional force that is only slightly affected by small clearance variations. The same holds for $k_{AR}(CS)$, as it results almost uniform over the cup surface, for the considered kinematic conditions. On the other hand, assuming $k_{AR}(CS, \bar{p})$, V results more sensitive to *cl* due to its dependence to the pressure.

On the other hand, for the PE law, the wear depth decreases only slightly with *cl* (indeed all wear maps are characterized by worn regions with similar green colors) and becomes more uniform. In fact, the red worn regions predicted for *cl*=0.04 mm at the edge of the contact area disappear for higher values of *cl*. Consequently, less conformal contacts lead to smaller worn areas affected by nearly the same wear depths, and thus to lower wear volumes. This can be explained by considering that, according to the PE law, the wear rate is not affected by the contact pressure and hence the effect of the contact conformity on wear depends only on the *CS*.

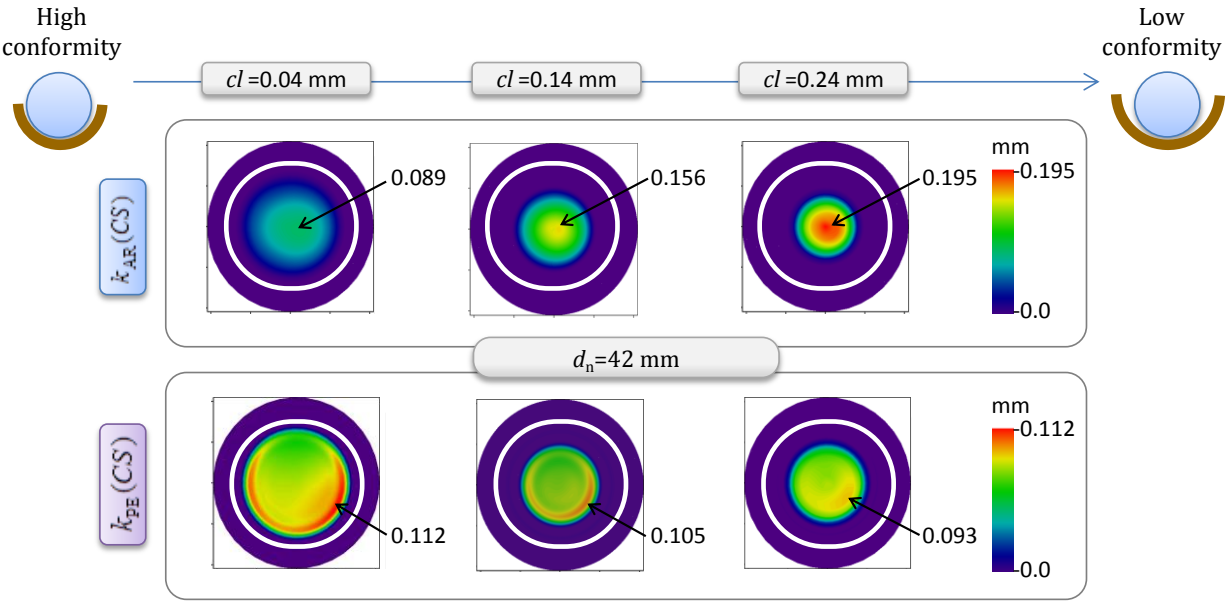

Fig.4. Comparison of the wear maps for 42 mm implants with increasing clearance. Results obtained for $k_{AR}(CS)$ (first row) and $k_{PE}(CS)$ (second row) are shown as examples. Note: The white line describes the border of the real humeral cup.

Results also demonstrated that the influence of wear laws/coefficients on wear predictions is important, in agreement with (Mattei et al. 2013b, Mattei et al. 2016).

For the AR law, the type of k function affects significantly the linear wear predictions but only slightly the wear volumes (Fig.3). The wear maps predicted for all k functions are qualitatively very similar, but they

differ quantitatively, especially for high values of *cl*. In fact, h_{max} for K_{AR} was higher than for $k_{AR}(CS)$, which in turn was higher than for $k_{AR}(CS, \bar{p})$, with maximum percentage difference of 26% and 67% for *cl*=0.24 mm, respectively. On the other hand, the maximum percentage variation of *V* was observed for the lowest *cl* and was limited to -14%.

As far as the wear law is concerned, the AR wear law predicted higher values of h_{max} with respect to the PE law (Fig.3a), for almost the whole range of *cl* value simulated, with percentage variation up to 54% ($h_{max}(K_{AR})$=0.203 mm vs $h_{max}(k_{PE}(CS))$=0.093 mm, at cl=0.24 mm). Only in the case of maximum conformity, the opposite ratio was observed, with a variation of h_{max} down to -24% ($h_{max}(K_{AR})$=0.091 mm vs $h_{max}(k_{PE}(CS))$=0.112, at cl=0.04 mm). The contrary is observed for *V* predictions (Fig.3b). Indeed, the PE law predicted higher values of *V* with respect to the AR law (up to 98%) for high conformities (*cl*<0.14 mm), whilst similar *V* were obtained for high *cl* (*cl*≥0.14 mm). It is worth noting that the wear law also affects the wear maps, as portrayed in Fig.4. Assuming the AR wear law, the cup surface was characterized by a central worn area with the maximum wear depth located at the cup dome, where the maximum contact pressure takes place throughout the wear cycle. On the other hand, according to the PE wear law, the wear depth was more uniform over the damaged surface, with maximum values located at the edge of the contact area.

3.2 Effect of implant size

The effect of implant size on wear is depicted in Figs.5 and 6.

Figure 5 describes the variation of h_{max} and *V* with the nominal diameter of RTSAs. It is worth noting that all implants were assumed to have the same *cl*, consequently, the higher d_n, the more conformal the contact. First of all, Fig.5b shows a distinct effect of implant size on *V* that is almost independent from wear law/coefficient: *V* increases with d_n from an average value of 22.6 to 26.6 mm³ (i.e. 18%).

On the other hand, as depicted in Fig.5a, the effect of d_n on h_{max} varies with the wear law. According to the AR law, the value of h_{max} remains almost constant while increasing d_n (maximum percentage variation from -2% to 6%), whilst, for the PE law, it increases with the implant size of about 24%. This is confirmed by the wear maps shown in Fig.6.

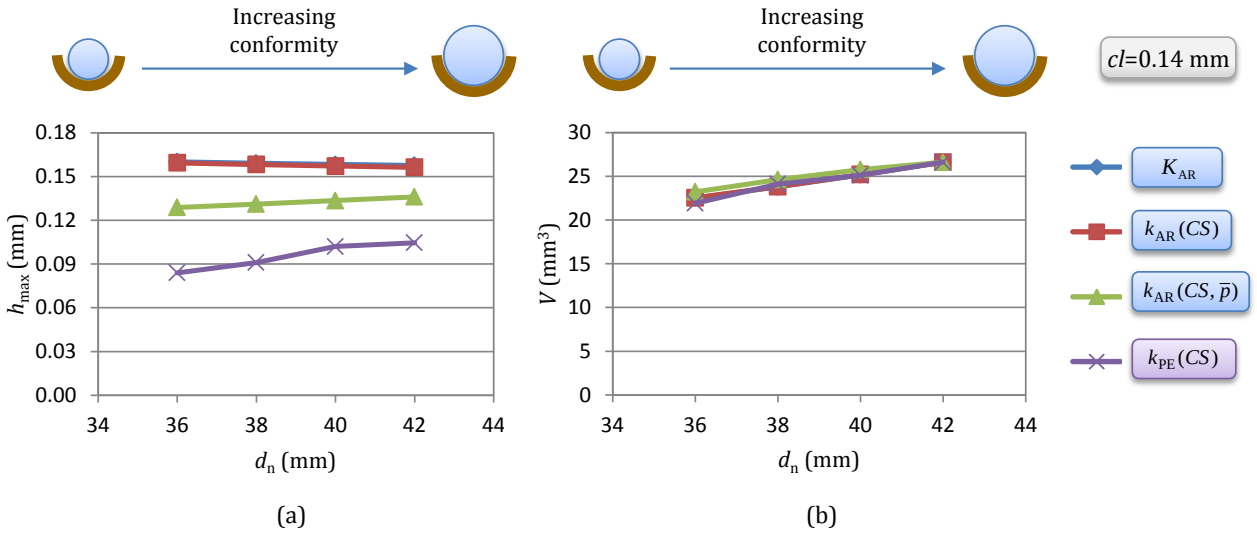

Fig.5. Effect of implant nominal diameter (d_n) on maximum wear depth (a) and wear volume (b), assuming cl=0.14 mm. Comparison of wear predictions for different wear laws and wear coefficients. Note that K_{AR} and $k_{AR}(CS)$ are overlapped in plot (a).

At the top of Fig.6, wear maps are predicted assuming $k_{AR}(CS)$ and different implant sizes. As can be seen, the results are very similar both qualitatively and quantitatively. It is worth noting that results obtained for $k_{AR}(CS)$ can be taken as a reference for the AR law, since they are very similar to those for K_{AR} and

$k_{AR}(CS, \bar{p})$ (as done in §3.1 and Fig.5). On the other hand, the linear wear predicted with the PE law and plotted at the bottom of Fig.6, is higher for larger implants, despite having similar spatial distribution for the different implant sizes with h_{max} located at the edge of the worn area. This can be observed, for instance, by comparing the regions in red colour that appear in the wear maps for d_n=40 and 42 mm.

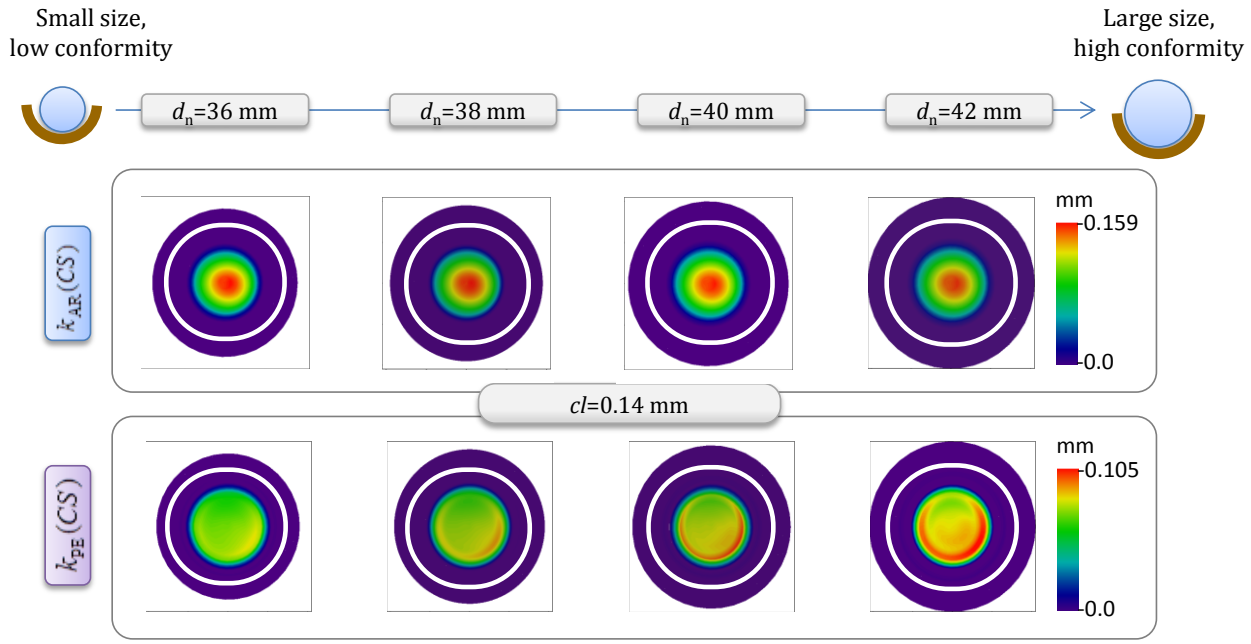

Fig.6. Comparison of the wear maps for implants with increasing diameter and cl=0.14 mm. Results obtained for $k_{AR}(CS)$ (first row) and $k_{PE}(CS)$ (second row) are shown as examples. As in Fig.4, the white line describes the border of the real humeral cup.

As far as the influence of the wear law/coefficient is concerned, results are in agreement with both §3.1 and (Mattei et al. 2013b, Mattei et al. 2016). Both the wear law and the wear coefficient mainly affect h_{max}. For all the implant sizes considered, similar values of h_{max} were obtained for K_{AR} and $k_{AR}(CS)$, higher than for $k_{AR}(CS, \bar{p})$ (% variation 15-24%), in turn higher than for $k_{PE}(CS)$ (% variation 30-53%). Such a difference was more marked for smaller implants.

4 Discussion

The important effect of the implant size and dimensional tolerance on wear of RTSAs has been proven by means of a large number of numerical simulations. However, such an effect depends on the wear law adopted. Indeed, given the open debate on the validity of the AR and the PE wear law for describing the wear of UHMWPE (Mattei et al. 2013b), all implant geometries were simulated using both laws and even considering different k functions. Summing up, it was noted that:

- For the AR law:
  - the higher the diametrical clearance the higher the maximum wear depth h_{max} (120%) while the lower the wear volume V (-9%);
  - as the nominal diameter d_n increases, the maximum wear depth h_{max} slightly decreases (-2%) while the wear volume V increases (18%);
- For the PE law:
  - Both the wear depth and volume have an inverse trend with respect to the diametrical clearance: when cl increases, h_{max} reduces up to -17% as well as V, up to -56%;
  - On the other side they both have the same trend of d_n: as the implant size increase h_{max} and V increase (24% and 21% respectively);

where percentage variations are computed comparing wear predictions for the limit values of the range of *cl* and d_n.

According to the AR wear law, a more precise tolerance, and hence a lower *cl*, guarantees a significant reduction of the linear wear to the detriment of a slight increase of *V,* which is in agreement with (Ribeiro et al. 2011). On the other hand, smaller implants are affected by lower wear volumes and almost unchanged h_{max}. Consequently, results suggest the best performing implants should have a small diameter and a tight dimensional tolerance. According to the PE wear law, a decrease of conformity (i.e. high *cl* and low d_n) causes a decrease of both linear and volumetric wear. In particular, very conformal implants can be affected by very high *V*. Thus, differently from the AR law predictions, the best performing implants would be small but with a certain clearance in between the head and cup surfaces. This conclusion reflects that the focus of our paper has been a computational wear model. However, we accept that the choice of an implant is a clinical decision which needs to be influenced by many factors, not only on wear. While, for example, a smaller implant can reduce wear, there may be negatives in terms of a reduced range of motion and reduced force necessary to dislocate the joint (Langohr et al. 2015). On the other hand, the different conclusions obtained from the two wear laws highlights the outstanding need for validating wear laws and hence wear models, as already discussed by the same authors (Di Puccio et al. 2015, Mattei et al. 2016).

However, it should be noted that, for both the wear laws, the dimensional tolerance influences the implant wear much more than the implant size, although it mainly affects h_{max} for the AR law and *V* for the PE law. Obviously, that is related to the range of *cl* and d_n values of practical interest. Indeed, the implant equivalent radius (according to the Hertzian theory) varies up to 300% and 30% when considering the effect of the clearance and size, respectively.

As a consequence, the dimensional tolerance plays a fundamental role on the wear of RTSAs, even though this parameter is neither specified in standards for RTSAs nor has ever been tackled in research studies. Thus, the present work suggests the insertion/specification of the value of dimensional tolerance in standards, as done for other implants (e.g. in ASTM F2033 for hip replacements (ASTM-International)), and perhaps the pursuing of more strict dimensional tolerances and, hence, a greater control/accuracy of the real implant dimension. It is also worth noting that the dimensional tolerance of the cup diameter measured in the present study, i.e. +0.2, -0.0 mm, is of the same order of magnitude of the linear wear. Another design parameter should be considered as it may affect the contact conditions, i.e. the geometrical tolerance. However, the measured samples were characterized by a sphericity deviation (of the radius) of 0.01 mm that is negligible with respect to the dimensional variation. As a concluding remark, there are some limitations of the present study. In addition to some critical points of the wear model examined in (Mattei et al. 2016), the main limitation consists in the values/expressions adopted for the wear coefficients. On the one hand, as discussed in the Introduction, such *k* functions (Table 1) represent an advancement with respect to the literature as they were estimated ad-hoc for RTSAs whilst other literature wear models (Terrier et al. 2009, Ribeiro et al. 2011, Quental et al. 2015) adopted *k* values of hip/knee implants. On the other hand, since *k* is a parameter very sensitive to the tested tribological conditions, it could also vary with the implant size and clearance, and not only with the implant type and the loading conditions. Accordingly, the values of *k* reported in Table 2 are theoretically valid only for the RTSAs geometry tested and simulated in (Mattei et al. 2016), having d_c=42.1 mm and *cl*=0.14 mm. However, the effect of the RTSAs geometry on *k* has never been addressed in the literature and the deepening of this matter would go beyond the aim of the present study. Consequently, all simulations, independently from implant geometry, were carried using the same *k* (Table 2). Future experimental and numerical studies will be devoted to overcome this limitation.

5 Conclusions

A sensitivity analysis of wear of RTSA to implant size and dimensional tolerance has been carried out using a numerical wear model. Ten different geometries were simulated assuming both the Archard wear law and a specific law for UHMWPE, and four different *k* functions, making 40 simulations in total. Two general conclusions were found. Firstly the best performing implant in terms of wear should be relatively small. Secondly a precise dimensional tolerance should be aimed for. Indeed, it was found that the clearance had a greater influence on wear than the change in implant diameter. Unfortunately, the two wear laws led to opposite conclusions regarding the implant conformity: the best performing implants should be very conformal for the AR law, but show little conformance according to the PE law.

This study has identified some points that might help in reducing wear and improving model reliability: a) the reduction of the dimensional tolerance range; b) the specification of implant dimensional tolerance in standards; c) the validation of wear laws/models; and d) the evaluation of the sensitivity of *k* to implant size and dimensional tolerance, hence to implant geometry.

6 References

[1] ASTM-International "ASTM 2033-05. Standard Specification for Total Hip Joint Prosthesis and Hip Endoprosthesis Bearing Surfaces Made of Metallic, Ceramic, and Polymeric Materials."

[2] Carpenter, S., D. Pinkas, M. D. Newton, M. D. Kurdziel, K. C. Baker and J. M. Wiater (2015). "Wear rates of retentive versus nonretentive reverse total shoulder arthroplasty liners in an in vitro wear simulation." Journal of Shoulder and Elbow Surgery.

[3] Day, J. S., D. W. MacDonald, M. Olsen, C. Getz, G. R. Williams and S. M. Kurtz (2012). "Polyethylene wear in retrieved reverse total shoulder components." Journal of Shoulder and Elbow Surgery **21**(5): 667-674.

[4] Di Puccio, F. and L. Mattei (2015). "A novel approach to the estimation and application of the wear coefficient of metal-on-metal hip implants." Tribology International **83**(0): 69-76.

[5] Dillon, M. T., C. F. Ake, M. F. Burke, A. Singh, E. H. Yian, E. W. Paxton and R. A. Navarro (2015). "The Kaiser Permanente Shoulder Arthroplasty Registry." Acta Orthopaedica **86**(3): 286-292.

[6] Fevang, B. T. S., S. A. Lie, L. I. Havelin, A. Skredderstuen and O. Furnes (2009). "Risk factors for revision after shoulder arthroplasty." Acta Orthopaedica **80**(1): 83-91.

[7] Kohut, G., F. Dallmann and U. Irlenbusch (2012). "Wear-induced loss of mass in reversed total shoulder arthroplasty with conventional and inverted bearing materials." Journal of Biomechanics **45**(3): 469-473.

[8] Kontaxis, A. (2010). Biomechanical analysis of reverse anatomy shoulder prosthesis. PhD, Newcastle University.

[9] Langohr, G. D. G., J. W. Giles, G. S. Athwal and J. A. Johnson (2015). "The effect of glenosphere diameter in reverse shoulder arthroplasty on muscle force, joint load, and range of motion." Journal of Shoulder and Elbow Surgery **24**(6): 972-979.

[10] Leslie, I., S. Williams, C. Brown, I. Graham, Z. M. Jin, E. Ingham and J. Fisher (2008). "Effect of bearing size on the long-term wear, wear debris, and ion levels of large diameter metal-on-metal hip replacements - An in vitro study." Journal of Biomedical Materials Research. Part B, Applied Biomaterials **87 (Pt B)**(1): 163-172.

[11] Liu, F., A. Galvin, Z. Jin and J. Fisher (2011). "A new formulation for the prediction of polyethylene wear in artificial hip joints." Proceedings of the Institution of Mechanical Engineers, Part H: Journal of Engineering in Medicine **225**(1): 16-24.

[12] Mattei, L., F. Di Puccio, B. Piccigallo and E. Ciulli (2011). "Lubrication and wear modelling of artificial hip joints: a review." Tribology International **44**(5): 532–549.

[13] Mattei, L. and F. Di Puccio (2013a). "Wear simulation of metal-on-metal hip replacements with frictional contact." Journal of Tribology **135**(2): 1-11.

[14] Mattei, L., F. Di Puccio and E. Ciulli (2013b). "A comparative study on wear laws for soft-on-hard hip implants using a mathematical wear model." Tribology International **63**: 66-77.

[15] Mattei, L., F. Di Puccio, T. J. Joyce and E. Ciulli (2016). "Numerical and experimental investigations for the evaluation of the wear coefficient of reverse total shoulder prostheses." Journal of the Mechanical Behavior of Biomedical Materials **55**: 53-66.

[16] Nam, D., C. K. Kepler, A. S. Neviaser, K. J. Jones, T. M. Wright, E. V. Craig and R. F. Warren (2010a). "Reverse Total Shoulder Arthroplasty: Current Concepts, Results, and Component Wear Analysis." The Journal of Bone & Joint Surgery **92**(Supplement 2): 23-35.

[17] Nam, D., C. K. Kepler, S. J. Nho, E. V. Craig, R. F. Warren and T. M. Wright (2010b). "Observations on retrieved humeral polyethylene components from reverse total shoulder arthroplasty." Journal of Shoulder and Elbow Surgery **19**(7): 1003-1012.
[18] Nyffeler, R. W., C. M. L. Werner, B. R. Simmen and C. Gerber (2004). "Analysis of a retrieved Delta III total shoulder prosthesis." Journal of Bone and Joint Surgery-British Volume **86b**(8): 1187-1191.
[19] Peers, S., J. E. Moravek, Jr., M. D. Budge, M. D. Newton, M. D. Kurdziel, K. C. Baker and J. M. Wiater (2015). "Wear rates of highly cross-linked polyethylene humeral liners subjected to alternating cycles of glenohumeral flexion and abduction." J Shoulder Elbow Surg **24**(1): 143-149.
[20] Quental, C., J. Folgado, P. R. Fernandes and J. Monteiro (2015). "Computational analysis of polyethylene wear in anatomical and reverse shoulder prostheses." Med Biol Eng Comput **53**(2): 111-122.
[21] Ribeiro, N. S., J. Folgado, P. R. Fernandes and J. Monteiro (2011). "Wear analysis in anatomical and reversed shoulder prostheses." Comput Methods Biomech Biomed Engin **14**(10): 883-892.
[22] Smith, S. L., B. L. Li, A. Buniya, S. H. Lin, S. C. Scholes, G. Johnson and T. J. Joyce (2015). "In vitro wear testing of a contemporary design of reverse shoulder prosthesis." Journal of Biomechanics **48**(12): 3072-3079.
[23] Terrier, A., F. Merlini, D. P. Pioletti and A. Farron (2009). "Comparison of polyethylene wear in anatomical and reversed shoulder prostheses." Journal of Bone & Joint Surgery, British Volume **91-B**(7): 977-982.
[24] Tudor, A., T. Laurian and V. M. Popescu (2013). "The effect of clearance and wear on the contact pressure of metal on polyethylene hip prostheses." Tribology International **63**(0): 158-168.
[25] Vaupel, Z. M., K. C. Baker, M. D. Kurdziel and J. M. Wiater (2012). "Wear simulation of reverse total shoulder arthroplasty systems: effect of glenosphere design." Journal of Shoulder and Elbow Surgery **21**(10): 1422-1429.
[26] Wiater, B. P., E. A. Baker, M. R. Salisbury, D. M. Koueiter, K. C. Baker, B. M. Nolan and J. M. Wiater (2015). "Elucidating trends in revision reverse total shoulder arthroplasty procedures: a retrieval study evaluating clinical, radiographic, and functional outcomes data." Journal of Shoulder and Elbow Surgery **24**(12): 1915-1925.